Lai, C.-S., Tooney, N. M., & Ankel, E. G. (1984) *Biochemistry 23*, 6393–6397.
Lakowicz, J. R. (1983a) *Principles of Fluorescence Spectroscopy*, pp 75–91, Plenum, New York.
Lakowicz, J. R. (1983b) *Principles* of *Fluorescence Spectroscopy*, pp 126–128, Plenum, New York.
Lorand, L., & Gotoh, T. (1970) *Methods Enzymol. 19*, 770–782.
March, J. C., Parikh, I., & Cuatrecasas, P. (1974) *Anal. Biochem. 60*, 149–152.
Miekka, S. I., Ingham, K. C., & Menache, D. (1982) *Thromb. Res. 27*, 1–14.
Mosesson, M. W., & Umfleet, R. A. (1970) *J. Biol. Chem. 245*, 5728–5736.
Mosesson, M. W., Chen, A. B., & Huseby, R. M. (1975) *Biochim. Biophys. Acta 386*, 509–524.
Narasimhan, C., & Lai, C.-S. (1989) *Biochemistry 28*, 5041–5046.
Odermatt, E., & Engel, J. (1989) in *Fibronectin* (Mosher, D. F., Ed.) pp 25–43, Academic Press, San Diego, CA.
Odermatt, E., Engel, J., Richter, H., & Hörmann, H. (1982) *J. Mol. Biol. 159*, 109–123.
Perrin, F. (1934) *J. Phys. 5*, 497–511.
Price, T. M., Rudee, M. L., Pierschbacher, M., & Ruoslahti, E. (1982) *Eur. J. Biochem. 129*, 359–363.
Provencher, S. W., & Glöckner, J. (1981) *Biochemistry 20*, 33–37.
Rawitch, A. B., Hudson, E., & Weber, G. (1969) *J. Biol. Chem. 244*, 6543–6547.
Rocco, M., Carson, M., Hantgan, R., McDonagh, J., & Hermans, J. (1983) *J. Biol. Chem. 258*, 14545–14549.
Rocco, M., Infusini, E., Daga, M. G., Gogioso, L., & Cuniberti, C. (1987) *EMBO J. 6*, 2343–2349.
Sjöberg, B., Pap, S., Österlund, E., Österlund, K., Vuento, M., & Kjems, J. (1987) *Arch. Biochem. Biophys. 255*, 347–353.
Smith, R. L., & Griffin, C. A. (1985) *Thromb. Res. 37*, 91–101.
Sober, H. A., Ed. (1970) *CRC Handbook of Biochemistry*, 2nd ed., pp J288–J291, Chemical Rubber Co., Cleveland, OH.
Tooney, N. M., Mosesson, M. W., Amrani, D. L., Hainfeld, J. F., & Wall, J. S. (1983) *J. Cell Biol. 97*, 1686–1692.
Wahl, P., & Weber, G. (1967) *J. Mol. Biol. 30*, 371–382.
Wall, J. S., Hainfeld, J. F., & Chung, K. D. (1985) in *Proceedings of the 43rd Annual Meeting of the Electron Microscopy Society of America* (Bailey, G. W., Ed.) pp 716–717, San Francisco Press, San Francisco, CA.
Weast, R. C., Ed. (1972) *CRC Handbook of Chemistry and Physics*, 53rd ed., F36, Chemical Rubber Co., Cleveland, OH.
Weber, G. (1952) *Biochem. J. 51*, 145–154.
Weber, G. (1953) *Adv. Protein Chem. 8*, 415–459.
Weber, G. (1981) *J. Phys. Chem. 85*, 949–953.
Weltman, J. K., & Edelman, G. M. (1967) *Biochemistry 6*, 1437–1447.
Williams, E. C., Janmey, P. A., Ferry, J. D., & Mosher, D. F. (1982) *J. Biol. Chem. 257*, 14973–14978.

Mechanism of Inhibition of the (Ca^{2+}–Mg^{2+})-ATPase by Nonylphenol†

F. Michelangeli,‡ S. Orlowski,§ P. Champeil,§ J. M. East,‡ and A. G. Lee*,‡
Department of Biochemistry, University of Southampton, Southampton SO9 3TU, U.K., and SBPH/DB and URA CNRS D1290, CEN Saclay, 91191 Gif-sur-Yvette Cedex, France

Received July 14, 1989; Revised Manuscript Received November 16, 1989

ABSTRACT: The effects of nonylphenol and 3,5-dibutyl-4-hydroxytoluene (BHT) on the activity of the (Ca^{2+}–Mg^{2+})-ATPase of skeletal muscle sarcoplasmic reticulum have been studied. At high concentrations, both inhibit the ATPase activity of the ATPase either in native lipid or in bilayers of dioleoylphosphatidylcholine but, at low concentrations, an increase in ATPase activity is observed, particularly for the ATPase reconstituted into dimyristoleoylphosphatidylcholine. Neither nonylphenol nor BHT binds at the lipid–protein interface of the ATPase. Nonylphenol decreases the effective equilibrium constant for phosphorylation of the ATPase by P_i probably through an increase in the effective rate of dephosphorylation of the phosphorylated ATPase. It also decreases the effective rate of the E2–Ca_2E1 transition and increases the effective equilibrium constant E2/E1 for the ATPase. Inhibition of ATPase activity follows from the slowing of the E2–E1 transition despite increases in effective rates for dephosphorylation and for the transport step, Ca_2E1P–E2P. Since nonylphenol has been shown to affect equilibrium constants for various steps in the reaction pathway of the ATPase, inhibition of activity of the ATPase cannot follow from effects on the fluidity (viscosity) of the membrane, since fluidity alone cannot affect equilibrium properties of the system.

The activities of many membrane proteins have been found to be affected by a wide range of hydrophobic molecules. Although some of these effects may arise from specific interactions between the hydrophobic additive and a distinct site on the protein, the majority of the effects are likely to be nonspecific. Since hydrophobic molecules partition extensively into the phospholipid component of biological membranes, effects of such molecules could follow from an effect on the fluidity of the bilayer, with the activity of membrane proteins being very sensitive to the fluidity, or viscosity, of the surrounding lipid (Sinensky, 1974; Chong et al., 1985; Almeida et al., 1986). To test this possibility, we previously studied the effect of lipid fluidity on the activity of the (Ca^{2+}–Mg^{2+})-ATPase purified from the sarcoplasmic reticulum of

† The SERC are thanked for financial support.
‡ University of Southampton.
§ SEN Saclay.

0006-2960/90/0429-3091$02.50/0

Scheme I

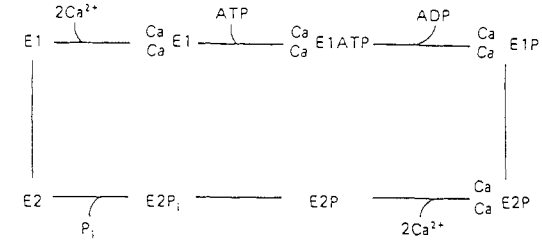

rabbit skeletal muscle. When we reconstituted the ATPase[1] into a series of phospholipid bilayers of different fluidities, we failed to find any correlation between ATPase activity and fluidity; what was important for the activity of the ATPase was the chemical structure of the surrounding phospholipid (East et al., 1984). We also found that the effects of hydrophobic additives could not be understood in any consistent way in terms of effects of fluidity. Thus, for example, cholesterol, which decreases the fluidity of lipid bilayers, either had no effect on the activity of the ATPase or caused a large increase in activity depending on the structure of the phospholipid present in the system (Simmonds et al., 1982). Fatty acids and long-chain alcohols, which increase the fluidity of lipid bilayers, had effects very similar to those of cholesterol (Froud et al., 1986a). We concluded therefore that effects of hydrophobic additives followed from direct interaction with the ATPase.

One region on a membrane protein such as the (Ca^{2+}–Mg^{2+})-ATPase where hydrophobic molecules could bind is at the lipid–protein interface. In previous papers we have shown that quenching of tryptophan fluorescence caused by molecules containing bromine could be used to determine binding to the ATPase; these studies showed that, as well as binding at the lipid–protein interface, other binding sites must be available on the ATPase for hydrophobic molecules, possibly at protein–protein interfaces in dimers or higher aggregates of the ATPase or between protein transmembrane helices (Lee et al., 1982; Simmonds et al., 1982; Froud et al., 1986b; Rooney et al., 1987). We also showed (Froud et al., 1986b) that it was possible to provide a partial explanation for the effects of hydrophobic molecules on the activity of the ATPase in terms of a kinetic model for the ATPase (Gould et al., 1986; Stefanova et al., 1987). The model is shown in simplified form in Scheme I and follows that of de Meis and Vianna (1979) in postulating two conformational states of the ATPase, E1 and E2. These two states differ in that the affinity for Ca^{2+} is high in the E1 conformation but low in the E2 conformation and in that the Ca^{2+} binding sites are exposed on the outer (cytoplasmic) side of the sarcoplasmic reticulum in E1 but exposed to the inside in E2. Following binding of Ca^{2+} and MgATP, the enzyme is phosphorylated and, after loss of MgADP, undergoes a conformation change to the E2P conformation from which Ca^{2+} is lost. Following hydrolytic cleavage of the phosphorylated intermediate, the enzyme recycles. Depending on the exact conditions, several steps in the sequence may be slow and partially rate controlling, including the E2–Ca_2E1 and Ca_2E1P–E2P transitions and the dephosphorylation step (Gould et al., 1986; Stefanova et al., 1987). As will be described later, a number of other important conformational changes also occur during the reaction cycle. We showed that the effects of a variety of hydrophobic molecules could be interpreted in terms of possible effects on the Ca_2E1P–E2P transition and dephosphorylation (Froud et al., 1986b).

Recently, Sokolove et al. (1986) reported that a series of lipophilic phenolic antioxidants were potent inhibitors of the (Ca^{2+}–Mg^{2+})-ATPase and were selective to the extent that they did not inhibit the mitochondrial F_1F_0–ATPase. Here we characterize in more detail the effects of phenols on the activity of the (Ca^{2+}–Mg^{2+})-ATPase.

Materials and Methods

4-Nonylphenol and 3,5-dibutyl-4-hydroxytoluene (BHT) were obtained from Fluka and Aldrich, respectively. Dioleoylphosphatidylcholine (DOPC) and dimyristoleoylphosphatidylcholine (DMPC) were obtained from Lipid Products and Avanti Polar Lipids, respectively. (Dibromostearoyl)phosphatidylcholine (BrPC) was prepared from DOPC as described in East and Lee (1982).

(Ca^{2+}–Mg^{2+})-ATPase was purified from sarcoplasmic reticulum of rabbit skeletal muscle as described in Froud et al. (1986a). The final preparation contained 30 phospholipid molecules/ATPase molecule, on the basis of a molecular weight of 110000 for the ATPase. A preparation of ATPase containing a higher molar ratio of phospholipid to ATPase was prepared by treatment of sarcoplasmic reticulum vesicles (SR) with low concentrations of deoxycholate as described by Meissner et al. (1973). ATPase activities were determined by using the coupled enzyme assay described in Froud et al. (1986a) in a medium, unless otherwise specified, containing 40 mM Hepes/KOH (pH 7.2), 5 mM $MgSO_4$, 2.1 mM ATP, 0.42 mM phosphoenolpyruvate, 0.15 mM NADH, 7.5 IU of pyruvate kinase, and 18 IU of lactate dehydrogenase in a total volume of 2.5 mL, with $CaCl_2$ and EGTA added to give ca. 10 μM Ca^{2+}; addition of further Ca^{2+} resulted in no increase in ATPase activity, establishing that this was a saturating concentration of free Ca^{2+}. In experiments where the Ca^{2+} concentration was varied, free Ca^{2+} concentrations were calculated by using the binding parameters given in Gould et al. (1986). Concentrations of protein were estimated by using the extinction coefficient given by Hardwicke and Green (1974).

SR was labeled with fluorescein 5′-isothiocyanate (FITC) at a ratio of FITC to ATPase of ca. 0.5:1 as described in Froud et al. (1986b). SR (0.6 mg) in buffer (35 μL; 50 mM potassium phosphate, 1 M KCl, and 0.25 M sucrose, pH 8) was incubated with FITC (2.5 nmol) added from a stock solution in dry dimethylformamide (5 mM). The reaction was left to stand at room temperature for 1 h and then diluted into buffer (250 μL; 50 mM Tris-HCl, pH 7, and 0.2 M sucrose), incubated for 30 min at 30 °C, and then kept on ice until use.

Lipid reconstitutions were carried out as described in Froud et al. (1986b). Lipid (1 μmol) was mixed with buffer (40 μL; 50 mM potassium phosphate, 1 M KCl, and 0.25 M sucrose, pH 8) containing $MgSO_4$ (5 mM), ATP (6 mM), and potassium cholate (12 mg/mL) and sonicated to clarity in a bath sonicator (Megason). ATPase (0.125 mg) in a volume of 3–10 μL was then added, and the mixture was left for 1 h at 5 °C to equilibrate before being diluted with buffer (200 μL) and stored on ice until use. For ATPase assays, samples (12 μL, equivalent to 6 μg of ATPase) were added to the assay mixture (2.45 mL) described above.

Fluorescence measurements were made in buffer (40 mM Hepes, 100 mM NaCl, and 1 mM EGTA, pH 7.2) by using a Perkin-Elmer LS-3B fluorometer. Tryptophan fluorescence

[1] Abbreviations: ATPase, (Ca^{2+}–Mg^{2+})-ATPase; BHT, 3,5-dibutyl-4-hydroxytoluene; BrPC, (dibromostearoyl)phosphatidylcholine; DMPC, dimyristoleoylphosphatidylcholine; DOPC, dioleoylphosphatidylcholine; FITC, fluorescein 5′-isothiocyanate; Hepes, 4-(2-hydroxyethyl)-1-piperazineethanesulfonic acid; Mes, 2-(*N*-morpholino)ethanesulphonic acid; SR, sarcoplasmic reticulum.

was excited at 295 nm and detected at 325 nm, with an ATPase concentration of 1.0 μM. Fluorescein fluorescence was excited at 495 nm and detected at 525 nm. For these experiments, labeled protein (20 μg) was added to buffer (2.5 mL; 50 mM Tris, 50 mM maleate, 5 mM $MgSO_4$, 100 mM KCl, and 100 μM EGTA) at the appropriate pH at 25 °C. The response to Ca^{2+} was determined by addition of a stock solution to give a final total concentration of 400 μM.

Steady-state measurements of enzyme phosphorylation by ATP were carried out in a medium of the following composition: 20 mM Hepes/Tris (pH 7.2), 5 mM $MgSO_4$, 100 mM KCl, 1 mM $CaCl_2$, and 0.1 mg/mL ATPase, in a total volume of 1 mL. The reaction was started by addition of [γ-^{32}P]ATP and, after incubation at 25 °C for 15 s, was quenched with ice-cold 25% trichloroacetic acid and 0.2 M potassium phosphate. The quenched protein was allowed to precipitate by incubating on ice for 15 min. The precipitate was collected by filtration through Whatman GF/C glass fiber filters, washed three times with 15 mL of cold 12% trichloroacetic acid and 0.2 M potassium phosphate, and finally counted in 4 mL of Labscint. A similar procedure was used to study phosphorylation of the ATPase by [^{32}P]P_i except that the buffer used was 150 mM Mes/Tris (pH 6.2), 10 mM $MgSO_4$, and 5 mM EGTA. The reaction was started by addition of between 1 and 10 mM P_i, at an ATPase concentration of 0.33 mg/mL. The reaction was quenched as described above after 15 s.

The time dependence of phosphorylation by [γ-^{32}P]ATP was determined by using the Biologic QFM-5 quench flow system. Sarcoplasmic reticulum was incubated with 0.04 g of the Ca^{2+} ionophore A23187 per gram of protein in 150 mM Mes/Tris pH 6, containing 20 mM $MgCl_2$ and 0.1 mM Ca^{2+}. This was mixed with an equal volume of 10 μM [γ-^{32}P]ATP at 20 °C, followed by quenching with the same volume of 1 M perchloric acid, 45 mM P_i, and 1.5 mM ATP.

The ratio of ADP-sensitive to ADP-insensitive forms of the ATPase was measured essentially as described by Shigekawa and Dougherty (1978). The ATPase (0.1 mg/mL) was incubated in buffer (1 mL; 20 mM Hepes/Tris, pH 7.2, 50 μM $MgSO_4$, 50 μM $CaCl_2$, and 100 μM KCl) at 0 °C. Phosphorylation was initiated by addition of 20 μM [γ-^{32}P]ATP, followed by incubation for up to 40 s. The maximal level of phosphorylation was established by quenching with 25% trichloroacetic acid and 0.2 M potassium phosphate. To establish the proportion of the phosphorylated ATPase in an ADP-reactive form, 50 μL of 2.5 mM ATP, 2.5 mM $MgSO_4$, and 30 mM ADP was added, followed by quenching 5–15 s later. The precipitated protein was filtered, washed, and counted as described above.

Calcium release from the ATPase at steady state in the presence of MgATP was determined as described by Champeil and Guillain (1986). The ATPase was adsorbed onto Millipore cellulose ester filters (HA 0.45 μm). An estimate of the amount of ^{45}Ca trapped in the filter with water but not bound to the ATPase was made by including [^{3}H]sucrose in the medium to allow a determination of the volume of solution trapped.

Binding of [^{14}C]ADP to the ATPase in 150 mM Mes/Tris, pH 6, 20 mM $MgCl_2$, and 2 mM EGTA was determined by Millipore filtration at 20 °C as described in Guillain et al. (1984).

Nonylphenol and BHT were generally added directly to the ATPase as concentrated solutions in methanol; methanol itself had no effect either on ATPase activity or on the fluorescence parameters at the concentrations employed. For the experiments with the reconstituted ATPase, nonylphenol or BHT was added to the initial lipid mixture in cholate used for the reconstitution.

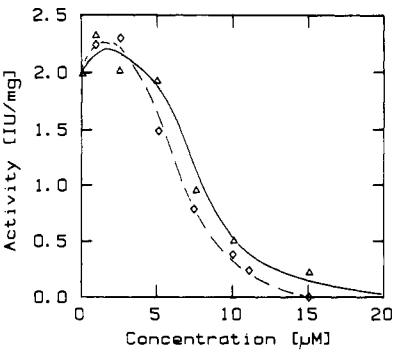

FIGURE 1: Effects of nonylphenol (◇) and BHT (△) on the ATPase activity (IU/milligram) of the purified ATPase (0.13 μM) in pH 7.2 buffer at 25 °C, assayed at saturating Ca^{2+} and an ATP concentration of 2.1 mM.

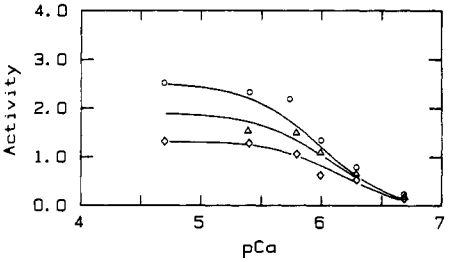

FIGURE 2: Effects of nonylphenol and BHT on the Ca^{2+} dependence of the activity (IU/milligram) of the purified ATPase, measured at pH 7.2 and 25 °C in the presence of 2.1 mM ATP and 0.13 μM ATPase: ATPase alone (○) and in the presence of 6 μM nonylphenol (◇) or 12 μM BHT (△). The lines are simulations with the parameters in Table III calculated as described in the text (for BHT with the rate of the E2–E1 transition for the MgATP-free and MgATP-bound forms equal to 0.4 and 33.0, respectively, with no effect on dephosphorylation or on the Ca_2E1P–E2P transition).

Kinetic simulations were carried out by using the FACSIMILE program (Chance et al., 1977) running on an IBM 3090 computer.

Results

As shown in Figure 1 addition of low concentrations of either nonylphenol or BHT to the purified (Ca^{2+}–Mg^{2+})-ATPase results in a small increase in ATPase activity, followed at higher concentrations by a marked decrease in activity. At an ATPase concentration of 0.1 μM, concentrations of nonylphenol and BHT causing 50% inhibition were 6 and 7 μM, respectively. As shown by Sokolove et al. (1986) for sarcoplasmic reticulum, the concentration of phenol required to give any particular level of inhibition increased with increasing protein concentration, indicating that a significant fraction of the phenol was bound to the membrane (data not shown). Inhibition of ATPase activity was reversible; addition of excess DOPC (80 μM) to the ATPase incubated with either 10 μM nonylphenol or 15 μM BHT for 20 min resulted in full restoration of activity (data not shown).

The effects of the phenols on the Ca^{2+} dependence of ATPase activity are shown in Figure 2. The phenols had no significant effect on the apparent affinity for Ca^{2+} in this experiment. Least-squares fits to the Hill equation showed no effect on the Hill coefficient n describing the cooperativity of Ca^{2+} binding, which was 1.7 both in the presence and in the absence of the phenols. It is known that the dependence of ATPase activity on the concentration of ATP is complex (Gould et al., 1986; Stefanova et al., 1987). Figure 3 shows

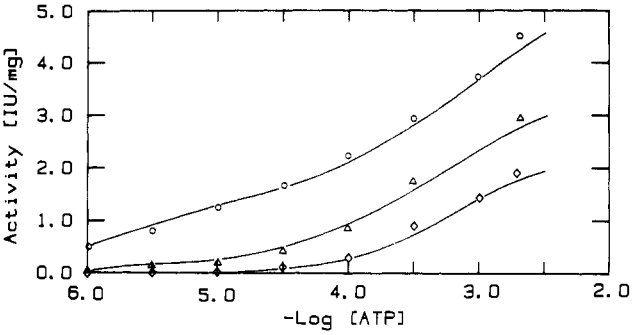

FIGURE 3: ATP concentration dependence of the activity of the purified ATPase at pH 7.2, 25 °C, with a saturating concentration of Ca^{2+} and 0.1 μM ATPase: ATPase alone (○) and in the presence of 6 μM nonylphenol (◇) or 10 μM BHT (△). The lines are simulations with the parameters in Table III for nonylphenol and for BHT with the rate of the E2–E1 transition for the MgATP-free and MgATP-bound forms equal to 0.4 and 33.0, respectively, with no effect on dephosphorylation or on the Ca_2E1P–E2P transition.

Table I: Phosphorylation of the ATPase with [γ-^{32}P]ATP[a]

concn of ATP (μM)	level of phosphorylation (nmol of EP/mg of protein) ATPase	ATPase + 20 μM nonylphenol	ATPase + 20 μM BHT
1.0	0.35	0.09	0.26
1.5	0.70		
2.5	1.48	0.52	0.61
5.0	2.09	0.78	1.48
20.0	3.13	1.91	3.04
100.0	3.56	2.26	3.04

[a] The ATPase (0.9 μM) was incubated with the given concentration of [γ-^{32}P]ATP for 15 s in the medium given under Materials and Methods containing 1 mM Ca^{2+} at pH 7.2, 25 °C, before quenching the reaction.

the effects of the phenols on ATPase activity as a function of ATP concentration; it is clear that inhibition of ATPase activity is more marked at low concentrations of ATP than at high concentrations.

To help distinguish between inhibition of ATPase activity at catalytic steps before or after phosphorylation of the ATPase, we determined the effect of the phenols on the maximal level of phosphorylation of the ATPase by [γ-^{32}P]ATP under conditions (1 mM Ca^{2+}) where the rate of dephosphorylation would be expected to be low. As shown in Table I, the maximal level of phosphorylation of the ATPase is considerably less than that expected if all the ATPase present were phosphorylated, the maximum ratio of phosphoenzyme to ATPase (3.5 nmol/mg in Table I) varying between preparations of the ATPase. Similarly low levels of phosphoenzyme formation have been reported by others (Coll & Murphy, 1984). The level of phosphoenzyme measured after a 15-s incubation decreased with decreasing concentrations of ATP, due to significant hydrolysis of the ATP even at the inhibitory concentrations of Ca^{2+} used in the experiment. As shown in Table I, addition of BHT had no significant effect on the level of phosphoenzyme formation, but addition of nonylphenol resulted in a significant reduction; as shown in Figures 4 and 6, much higher concentrations of nonylphenol or different experimental conditions resulted in a much reduced or almost zero level of phosphoenzyme at steady state. Measurement of the time course of phosphorylation of the ATPase (Figure 4) showed that nonylphenol did not prevent the formation of phosphoenzyme at short times after the addition of ATP but that the level of phosphoenzyme rapidly declined to give, for a high concentration of nonylphenol, a very low level of phosphoenzyme in the steady state. As shown in Figure 5,

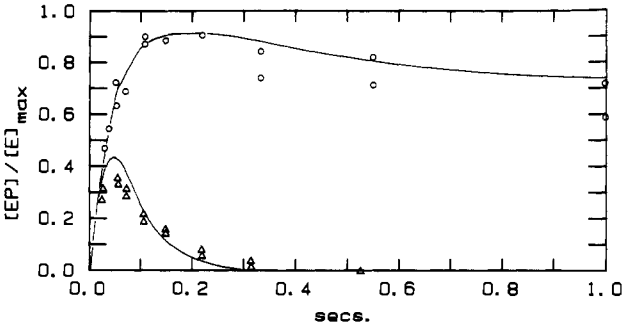

FIGURE 4: Rate of phosphorylation of SR (0.1 mg of protein/mL) by 5 μM [γ-^{32}P]ATP in the presence of A23187 at pH 6, 20 mM Mg^{2+}, 0.1 mM Ca^{2+}, 20 °C, in the absence (○) or presence (△) of 100 μM nonylphenol. The experimental data are expressed as $[EP]/[EP]_{max}$, assuming a value for $[EP]_{max}$ of $0.6[E]_{total}$ (EP_{max} = 5.2 nmol/mg of protein). The lines are simulations with the parameters in Table III but with 20- and 15-fold increases in the rates of the Ca_2E1P–E2P transition and dephosphorylation, respectively, as described in the text.

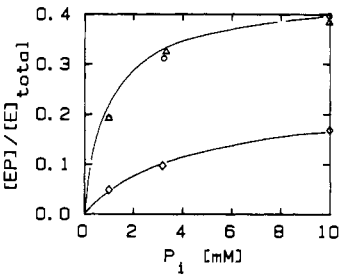

FIGURE 5: Equilibrium phosphoenzyme level for the purified ATPase (2.9 μM) at pH 6.2, 25 °C, as a function of phosphate concentration, for the ATPase alone (○) or in the presence of 12 μM nonylphenol (◇) or 25 μM BHT (△). Experimental data are expressed as $[EP]/[EP]_{total}$, assuming a value for $[EP]_{max}$ of $0.5[E]_{total}$. The lines are simulations with the parameters given in Froud and Lee (1986), with an effective equilibrium constant (pH 6.2, no K^+) K_A for phosphorylation of 14.3 in the absence of nonylphenol and 1.9 in its presence.

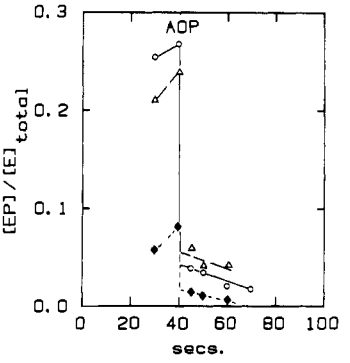

FIGURE 6: Dephosphorylation by ADP of phosphoenzyme formed from the purified ATPase (0.7 μM) and ATP at pH 7.2, 50 μM $MgSO_4$, 50 μM $CaCl_2$, and 100 μM KCl at 0 °C. After incubation of the ATPase with 20 μM [γ-^{32}P]ATP for 40 s, ADP (final concentration 1.5 mM) was added, and the level of phosphoenzyme remaining was determined. The ratio of ADP-sensitive to ADP-insensitive phosphoenzyme was determined by extrapolation, as shown; ATPase alone (○) or in the presence of 20 μM nonylphenol (◆) or 20 μM BHT (△).

nonylphenol also causes a significant reduction in the level of phosphoenzyme formed from [^{32}P]P_i, with BHT having no significant effect.

Shigekawa and Dougherty (1978) have shown that it is possible to estimate the relative proportions of ADP-sensitive and ADP-insensitive ATPase by first phosphorylating the ATPase with [γ-^{32}P]ATP and then measuring the level of

Table II: Levels of Ca^{2+} Bound to the ATPase[a]

	Ca^{2+} bound (nmol/mg)			
	pH 6		pH 7.2[b]	
system	expt	calc[c]	expt	calc[c]
no nonylphenol				
no ATP	10.2	10.4	9.8	10.4
+500 μM ATP	3.7	4.1	7.5	8.8
60 μM nonylphenol				
no ATP	6.2	10.4	6.7	10.4
+500 μM ATP	0.9	0.6	2.5	1.1

[a] 20 °C, 20 mM Hepes/Tris, 5 mM $MgSO_4$, 50 μM $CaCl_2$, with 0.1 mg of ATPase adsorbed per filter. Experimental levels of bound Ca^{2+} corrected for a level of nonreleasable Ca^{2+} of 0.7 nmol/mg of protein. [b] Buffer also contained 100 mM KCl. [c] Calculated by assuming 60% activity for the ATPase, with rate parameters as given in Table III for ATPase activity data (Figure 3; ATPase = 0.1 μM, nonylphenol = 6 μM).

phosphorylation as a function of time following the addition of ADP. The result of such an experiment at 0 °C is shown in Figure 6. It is clear that under the conditions of the experiment the phosphorylated ATPase is predominantly in an ADP-sensitive form and that although the addition of nonylphenol decreased the level of phosphoenzyme, the phosphoenzyme remained predominantly ADP sensitive.

Information about the relative proportions of Ca^{2+}-bound and Ca^{2+}-free forms of the ATPase at steady state in the presence of MgATP can also be obtained by measurement of the Ca^{2+} released on addition of MgATP (Champeil & Guillain, 1986). In the absence of MgATP and presence of Ca^{2+}, the ATPase will be in the Ca_2E1 form. On addition of ATP, following phosphorylation of the ATPase and the Ca_2E1P–E2P step, E2P will have been formed, from which Ca^{2+} will have been released. The magnitude of the Ca^{2+} released is a measure of the proportion of the ATPase in the E2P or E2 forms. As shown in Table II, Ca^{2+} release on addition of MgATP is greater at pH 6 than at pH 7, as previously reported (Champeil & Guillain, 1986). Addition of nonylphenol results in almost total release of Ca^{2+} on addition of MgATP, suggesting that at steady state the ATPase is predominantly in the E2 or E2P forms.

Information about the E2–E1 conformational change for the ATPase can be obtained from studies of the fluorescein fluorescence of the ATPase covalently modified with fluorescein isothiocyanate. Pick (1982) has shown that addition of Ca^{2+} to the modified ATPase results in a small decrease in fluorescein fluorescence that can be attributed to the E2–E1 conformational change (Pick, 1982; Froud et al., 1986b). As shown in Figure 7, the magnitude of the fluorescence change on addition of Ca^{2+} is increased by addition of nonylphenol or BHT at pH 7. Further, whereas the rate of the transition is markedly decreased by addition of nonylphenol at pH 6 or pH 7, addition of BHT has no detectable effect on the rate.

Significant increases in tryptophan fluorescence of the ATPase occur on addition of Ca^{2+} to the ATPase, which have been attributed to a conformational change on the ATPase following the binding of the first Ca^{2+} and before the binding of the second Ca^{2+}, that is, to the CaE1–CaE1′ transition (Fernandez-Belda et al., 1984). Figure 8 shows that addition of nonylphenol causes a significant shift in the Ca^{2+} concentration dependence of this transition to higher Ca^{2+} concentrations, together with an increase in the magnitude of the fluorescence change. Addition of nonylphenol to the ATPase results in a reduction in the fluorescence of the ATPase either in EGTA or in saturating Ca^{2+}, but with the former change being greater (data not shown); this results in the observed

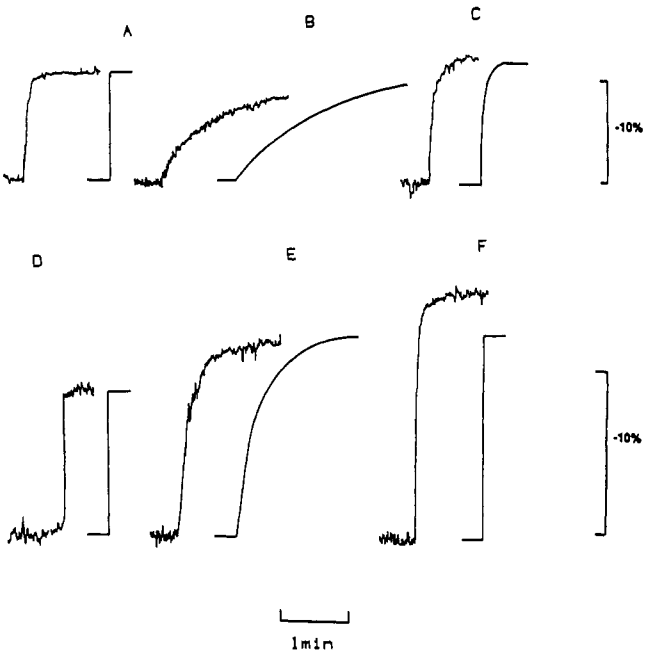

FIGURE 7: Changes in fluorescence intensity for FITC-labeled SR caused by the addition of Ca^{2+} to a final concentration of 400 μM for SR (0.18 μM) in buffer containing 100 μM EGTA either alone (A, D) or in the presence of 10 μM nonylphenol (B, E) or 10 μM BHT (C, F) at pH 6 (A–C) or pH 7 (D–F). An upward deflection here represents a decrease in intensity. To the right of each experimental curve is the corresponding simulation calculated as described in the text.

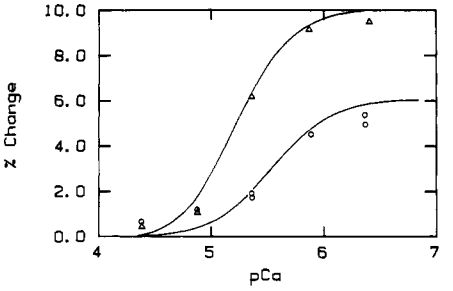

FIGURE 8: Percent decrease in tryptophan fluorescence intensity of the purified ATPase (0.9 μM) at pH 7.2 in the absence (○) or presence (△) of 60 μM nonylphenol, as a function of the free Ca^{2+} concentration. The lines are simulations calculated as described in the text, with a 7-fold increase in the E2/E1 equilibrium constant on addition of nonylphenol.

increase in the fluorescence response to Ca^{2+}.

Phosphorylation of the ATPase by ATP in the presence of Ca^{2+} has been shown to cause a small transient decrease in tryptophan fluorescence intensity which is reversed when the added ATP is hydrolyzed (Figure 9; Dupont, 1978; Champeil et al., 1986). In the presence of nonylphenol the fluorescence response to addition of MgATP is longer lived, as expected from the reduced ATPase activity, but is also very much larger. Addition of BHT has similar effects, although not as marked (data not shown).

The importance of lipid structure for the effect of phenols on ATPase activity is illustrated in Figure 10. The ATPase was reconstituted into bilayers of defined composition by incubation of the ATPase with a 1000-fold excess of the test lipid, followed by a 1200-fold dilution into buffer to dissociate the cholate from the lipid–protein complex (Froud et al., 1986b). When assayed at 25 °C, saturating Ca^{2+} concentration, and an ATP concentration of 2.1 mM, the ATPase activity for the ATPase reconstituted with DOPC was found to be greater than that for the ATPase reconstituted with the

Table III: Kinetic Parameters Obtained by Simulation for the (Ca^{2+}–Mg^{2+})-ATPase at 25 °C, pH 7.2 (Rates Expressed as s^{-1})

	nonylphenol[a] (μM)		nonylphenol[b] (μM)				
step	0	6	0	20	40	60	70
E2–E1	2×10^3	0.07	2×10^3	0.07	0.07	0.07	0.07
E1–E2	2.9×10^3	0.68	2.9×10^3	0.68	0.68	0.68	0.68
E2MgATP–E1MgATP[d]	2×10^3	5.66	2×10^3	198.2	49.6	24.8	16.5
E1MgATP–E2MgATP	8.1	0.42	8.1	43.3	10.8	5.42	3.61
Ca_2E1P–Ca_2E2P[c]	6.9	68.7	5.3	5.3	52.7	52.7	52.7
Ca_2E1PMgATP–Ca_2E2PMgATP	54.9	549.2	175.7	175.7	1757.4	1757.4	1757.4
E2PMg–E2PiMg[e]	19.2	134.7	57.5	57.5	402.4	402.4	402.4

[a] ATPase activity data Figure 3; K^+ = 12 mM, Mg^{2+} = 5 mM, ATPase = 0.1 μM, purity = 60%. Rate parameters for Figure 2 as listed, except for Ca_2E1PMgATP–Ca_2E2PMgATP, which are equal to 34.3 and 343.2 in the absence and presence of nonylphenol, respectively. Rate parameters for Figure 4 as listed, except for Ca_2E1PMgATP–Ca_2E2PMgATP, which are equal to 34.3 and 686.5 in the absence and presence of nonylphenol, respectively, and E2PMg–E2PiMg, which are equal to 3.0 and 45.0 in the absence and presence of nonylphenol, respectively, under the conditions of this experiment (pH 6). [b] Tryptophan fluorescence data Figure 9; K^+ = 100 mM, Mg^{2+} = 5 mM, ATPase = 1 μM, purity = 50%. [c] Assumed to be a slow step, see text. [d] Binding constant of MgATP to E2 = 0.5 mM. [e] Rate constant for MgATP-bound forms assumed to be 1.5 times those of the MgATP-free forms.

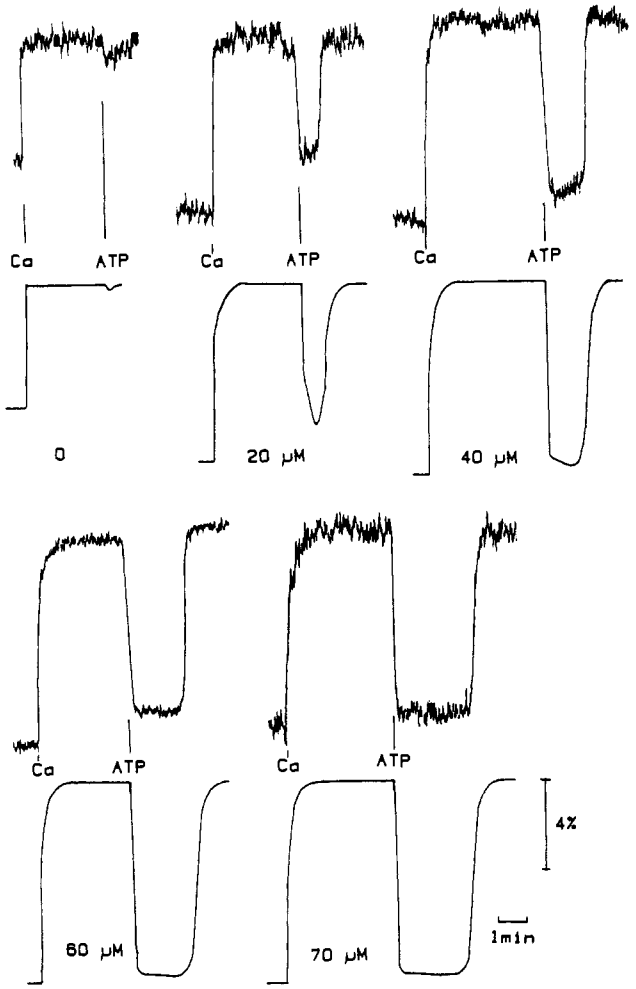

FIGURE 9: Effect of addition of calcium (final concentration 250 μM) or ATP (final concentration 20 μM) on the tryptophan fluorescence intensity of the purified ATPase (1 μM) in buffer containing 25 μM EGTA in the absence of nonylphenol or in the presence of nonylphenol at the given concentrations, at pH 7.2. The upper curves are experimental, and the lower curves are simulations with the parameters in Table III and calculated as described in the text.

short-chain phospholipid DMPC (Figure 10). Addition of either BHT or nonylphenol to the ATPase reconstituted with DOPC had only a small stimulatory effect on activity up to a molar ratio of phenol to lipid of 0.4:1, beyond which ratio the effect on activity was inhibitory. In contrast, addition of the phenols to the ATPase reconstituted with DMPC resulted in a large increase in activity to a maximal value at a molar ratio of phenol to lipid of 0.8:1, beyond which ratio inhibition was observed. The maximal stimulated rate observed in the

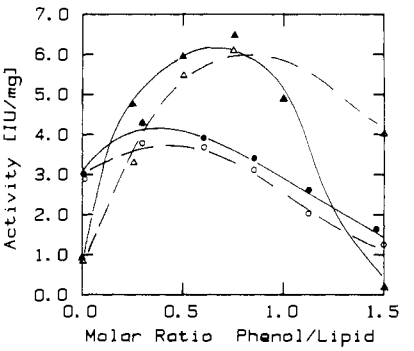

FIGURE 10: Effect of the addition of nonylphenol (▲, ○) or BHT (△, ●) at the given molar ratios of phenol to phospholipid on the activity (IU/milligram) of the purified ATPase reconstituted with dioleoylphosphatidylcholine (●, ○) or dimyristoleoylphosphatidylcholine (▲, △). [MgATP] = 2.1 mM, pH 7.2, 25 °C.

Table IV: Effect of Nonylphenol and BHT on Tryptophan Fluorescence of the ATPase Reconstituted with BrPC[a]

	relative fluorescence intensity[b]	
molar ratio phenol/lipid	nonylphenol	BHT
0	0.42	0.42
0.35	0.44	0.42
1.0	0.42	0.39

[a] The purified ATPase (0.065 μM) was reconstituted with BrPC at a phospholipid: ATPase molar ratio of 900:1. [b] Measured relative to that of the ATPase reconstituted with DOPC.

DMPC–ATPase system was about twice that seen in the DOPC–ATPase system, despite the fact that the unstimulated rate is considerably less in the DMPC–ATPase system than in the DOPC–ATPase system.

In previous publications we have shown that the ability of hydrophobic molecules to bind at the lipid–protein interface of the ATPase could be determined from their effect on the tryptophan fluorescence of the ATPase reconstituted with the quenching lipid BrPC (East & Lee, 1982). Reconstitution of the ATPase with BrPC results in a decrease in tryptophan fluorescence intensity to ca. 40% of that seen for the ATPase reconstituted with DOPC. Addition of any nonquenching hydrophobic molecule that can bind at the lipid–protein interface results in an increase in fluorescence intensity for the BrPC–ATPase system as a result of displacement of BrPC from the surface of the ATPase (East & Lee, 1982; de Foresta et al., 1989). As shown in Table IV addition of neither nonylphenol nor BHT had any effect on the fluorescence of the BrPC–ATPase system, indicating no significant binding of the phenols at the lipid–protein interface at up to a molar ratio of phenol to lipid of 1:1.

Discussion

Despite much work there is still little clear idea as to how hydrolysis of ATP is linked to the transport of an ion such as Ca^{2+} across the biological membrane. The majority of experiments on the kinetics of the (Ca^{2+}–Mg^{2+})-ATPase have been interpreted in terms of the E1/E2 model shown in Scheme I, which proposes two major conformational states E1 and E2 for the ATPase, differing in the affinity and orientation of the Ca^{2+} binding sites (de Meis & Vianna, 1979). Stahl and Jencks (1987), however, have argued against the E1/E2 model and have suggested that dephosphorylation of the phosphorylated ATPase can lead directly to a species whose transport sites face the cytoplasm, without any need for an intermediate E2 form. One approach to defining the mechanism of the ATPase is to study the effects of inhibitors that may, in fortunate cases, so decrease the rate of some normally fast step in the sequence as to make it a rate-controlling step and so amenable to study.

Sokolove et al. (1986) have shown that the addition of nonylphenol and BHT at high concentrations inhibits the ATPase activity of the ATPase, although at low concentrations their addition results in a small increase in activity (Figure 1); a similar pattern of effects has been observed for a variety of alcohols (Jones & Lee, 1986; Froud et al., 1986b). The phenols are particularly suited to a detailed study of the mechanism of inhibition, both because the inhibitory effects are greater than seen with the alcohols (Froud et al., 1986b) and because the phenols are sufficiently water soluble to partition directly into the membrane when added to a membrane suspension.

In comparing the various experiments, account has to be taken of the very different protein concentrations employed for the different measurements. From the parameters of Leo et al. (1971) the oil–water partition coefficient K_p (in units of moles per liter of solvent) of nonylphenol can be estimated to be 800 000, so that under the conditions of our experiments partition of nonylphenol into the lipid bilayer component of the membrane will be highly favored. Comparisons between experiments are therefore best made in terms of the molar ratio of phenol to ATPase, rather than in terms of the aqueous concentration of phenol. Measurements of light scattering by liposomes of dioleoylphosphatidylcholine show only small changes on addition of nonylphenol up to a molar ratio of nonylphenol to phospholipid of 0.4:1, but beyond this ratio (at lipid concentrations between 50 and 200 μM) very large changes in light scattering occur, indicating some major change in the organization of the system (data not shown). For the purified ATPase, the molar ratio of phospholipid to ATPase is 30:1, so that effects of nonylphenol on ATPase activity (Figure 1) occur at molar ratios of nonylphenol to phospholipid where large changes in lipid organization are likely to have occurred.

The effects of nonylphenol on ATPase activity do not follow from simple competitive inhibition. Although addition of nonylphenol results in a decrease in the affinity of the ATPase for Ca^{2+} (Figure 8), this can, as described later, be attributed to a decrease in the equilibrium constant E1/E2, which has no significant effect on the Ca^{2+} dependence of activity (Figure 2; see below). Also as will be shown later, and in agreement with Sokolove et al. (1986), effects are inconsistent with any major change in the affinity for MgATP.

In general, inhibition for any step E^a–E^b in the reaction sequence of the ATPase resulting from binding of a hydrophobic molecule such as nonylphenol (which is likely to be able to bind to multiple sites on the ATPase) which is not competitive can be represented by

$$\begin{array}{ccc} E^a & \rightleftharpoons & E^b \\ \Updownarrow & & \Updownarrow (i = 1\text{–}n) \\ E^aN_i & \rightleftharpoons & E^bN_i \end{array}$$

where N represents nonylphenol and up to n mol of nonylphenol can bind per mole of ATPase. Possible modes of inhibition are described, for example, in Segal (1975; see especially Chapters 4 and 8). Inhibition could follow from a slower rate for E^aN_i–E^bN_i than for E^a–E^b [analogous to classical partial noncompetitive inhibition (Segal, 1975)]. If the effects of binding of nonylphenol were equal on the forward and back rate constants, then the equilibrium constants E^aN_i/E^bN_i would equal that for E^a/E^b, and nonylphenol would bind equally to E^a and E^b. Alternatively, binding of nonylphenol could affect the forward and back rate constants for the transition differently, so that the equilibrium constants E^aN_i/E^bN_i would no longer equal that for E^a/E^b, and thus nonylphenol would bind with different affinities to E^a and E^b. We will give examples below where binding of nonylphenol does affect equilibrium constants for steps of the reaction cycle (e.g., that for phosphorylation from P_i) so that differential binding of nonylphenol to different forms of the ATPase must occur. In the extreme, the rate of the E^aN_i–E^bN_i transition might be zero for some or all of the possible values of i, corresponding to classical noncompetitive inhibition (Segal, 1975). In all cases, at any particular concentration of nonylphenol, the measured rate for any particular step will be an appropriately weighted sum of the rates for all the n nonylphenol-bound species present; if it can be assumed that the on- and off-rate constants describing the binding of nonylphenol to the ATPase are fast, and if it can be assumed that any conformational changes on the ATPase that follow from the binding of nonylphenol are also fast, then the appropriate weighting will simply be the relative proportions of the ATPase in the various nonylphenol-bound forms as calculated from the binding constant for nonylphenol [the quasi-equilibrium approach; see Cha (1968)]. For nonylphenol, where multiple binding to the ATPase is expected (see below), no detailed analysis of binding of nonylphenol to the ATPase is possible, so that calculation of specific rate constants for each of the n possible nonylphenol-bound states of the ATPase is not possible nor is it required for the analysis given below. Rather, we have attempted simply to identify which steps in the reaction sequence are altered by binding of nonylphenol, and we give "effective" rate constants for these steps in the presence of given concentrations of nonylphenol.

The studies reported here restrict the inhibitory effects of nonylphenol to just two possible steps in the reaction sequence. The observation that the level of phosphorylated ATPase at steady state in the presence of ATP is reduced by the addition of nonylphenol (Figure 4; Table I) shows that inhibition of ATPase activity must follow from a decrease in the effective rate of some step either before phosphorylation or after dephosphorylation, since a decrease in the effective rate of any other step would lead to an increase in the proportion of the ATPase in a phosphorylated form at steady state in the presence of ATP. The observation that, at steady state in the presence of ATP, the ATPase is predominantly present in a Ca^{2+}-free form (Table II; Figure 9) further restricts the inhibition to a step following dephosphorylation and before the binding of Ca^{2+}, that is, in terms of Scheme I, to either the E2–E1 step or to the binding of Ca^{2+} to E1 to give Ca_2E1. The further observation that inhibition of ATPase activity is more marked at low concentrations of MgATP than at high

concentrations (Figure 3) suggests either a very marked decrease in the affinity of the ATPase for MgATP or a decrease in the rate of one or more of the steps stimulated by MgATP.

These arguments can be put more quantitatively in terms of a full kinetic model for the ATPase based on the two-conformation model of de Meis and Vianna (1979) (Gould et al., 1986; Stefanova et al., 1987; Scheme I). As well as the E1 and E2 conformational states, a number of other conformational states have to be introduced. To explain the cooperativity of Ca^{2+} binding, it is necessary to postulate a slow conformational change CaE1–CaE1′ between binding of the first and second Ca^{2+} ions (Gould et al., 1986). The activity of the ATPase is sensitive to pH, with an optimum at about pH 7.2. In Gould et al. (1986) this was attributed to decreases in the rates of dephosphorylation and of the Ca_2E1P–Ca_2E2P step at low and high pH, respectively. Champeil and Guillain (1986) and Wakabayashi et al. (1986), however, have shown that the rate of the Ca_2E1P–E2P change is not very dependent on pH, and Bishop and Al-Shawi (1988) have shown that the effect of high pH is very dependent on the concentration of Mg^{2+}. We have therefore modified the kinetic model, removing the suggested pH dependence of the Ca_2E1P–Ca_2E2P transition and now attributing the decrease in activity at high pH to the binding of Mg^{2+} to the Ca^{2+} binding sites on E2P, with binding of Mg^{2+} at these sites, like Ca^{2+}, reducing the rate of dephosphorylation (Michelangeli, East, and Lee, unpublished results). The steady-state ATPase activity measurements and the data reported here are consistent with the Ca_2E1P–E2P change being relatively slow and partly rate controlling, with the slow step being either Ca_2E1P–Ca_2E2P or the loss of Ca^{2+} from Ca_2E2P. Stahl and Jencks (1987) have shown the presence of a conformational change between binding of MgATP to Ca_2E1 and phosphorylation, which has also been incorporated into the model. It has been suggested that the dependence of ATPase activity on the concentration of MgATP is complex (Figure 3) because MgATP can bind to both E1 and Ca_2E1P, increasing the rate of the Ca_2E1P–E2P transition; the apparent affinity of Ca_2E1P for MgATP is in the millimolar range, compared to a micromolar affinity of E1 for MgATP [see references in Gould et al. (1986)]. Binding of MgATP to E1 has also been suggested to increase the rates of the CaE1–CaE1′ and E2–E1 transitions and of dephosphorylation [see references in Gould et al. (1986), Stefanova et al. (1987), and Lee (1987)].

The possibility that the observed decrease in ATPase activity caused by nonylphenol follows from a decrease in the affinity of the ATPase for MgATP can readily be eliminated. The observed effect of nonylphenol on the MgATP dependence of ATPase activity (Figure 3) can be simulated reasonably well by assuming a decrease in the affinity of the ATPase in the Ca_2E1 form from 3.6 to 200 μM, but such a decrease in affinity would result in a very marked reduction in the rate of phosphorylation of the ATPase by 5 μM MgATP. Simulations show that the expected time to reach 50% of the maximal level of phosphorylation would increase from 30 ms in the absence of nonylphenol to 250 ms in its presence; the experimental data show no significant effect on the rate of phosphoenzyme formation (Figure 4). Further, although these simulations show a decrease in the level of maximum phosphorylation to $[EP]_{max}/[E]_{total}$ of 0.32, comparable to the observed value of 0.35, they show that this maximal level of phosphorylation would be maintained for over 2 s, whereas, in fact, a very rapid decay of phosphoenzyme is observed (Figure 4). Finally, we carried out direct measurements of binding of MgADP to Ca_2E1 and observed identical binding

Scheme II

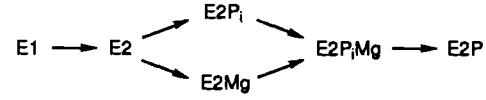

in the presence and absence of 40 μM nonylphenol, the concentration of MgADP for half-saturation being 30 μM in the presence of 20 mM Mg^{2+} at pH 6.0 (data not shown).

As described above, the slow step in the presence of nonylphenol must be a step following dephosphorylation and before phosphorylation and one stimulated by MgATP. There are two such potential steps, the E2–E1 and CaE1–CaE1′ transitions. However, the affinity of E1 for MgATP is in the micromolar range and, correspondingly, the concentration of MgATP increasing the rate of the CaE1–CaE1′ transition is also in the micromolar range (Gould et al., 1986). Not surprisingly, therefore, we have been unable to simulate the experimentally determined dependence of ATPase activity on MgATP concentration (Figure 3) in terms of a decrease in the rate of the CaE1–CaE1′ transition. This then leaves the E2–E1 transition as a possible target for inhibition.

The effect of nonylphenol on phosphorylation of the ATPase by P_i (Figure 5) and the rapid loss of phosphoenzyme observed after phosphorylation by MgATP in the presence of nonylphenol (Figure 4) show that steps other than the E2–E1 transition must also be modified by nonylphenol, and indeed, simulations show that the relative degrees of inhibition of ATPase activity at high and low concentrations of MgATP cannot be matched well by assuming effects only on the rate of the E2–E1 step. Phosphorylation of the ATPase by P_i can be described in terms of Scheme II. Effective equilibrium constants for each of the steps are calculated as given in Froud and Lee (1986). At pH 6.2 in the absence of K^+, the effective equilibrium constant for phosphorylation [K_A in Froud and Lee (1986)] is 14.3, and, as shown in Figure 5, this gives a good fit to the data obtained here, either for the ATPase alone or for the ATPase in the presence of BHT. The decreased level of phosphorylation in the presence of nonylphenol is consistent with a decrease in the effective equilibrium constant for phosphorylation to 1.9 (Figure 5) Such a decrease in the effective equilibrium constant for phosphorylation suggests an increase in the rate constant for dephosphorylation, consistent with the rapid decrease in the phosphoenzyme level observed in the presence of nonylphenol (Figure 4). Simulations show, however, that the rate of the Ca_2E1P–E2P transition (2.1 s^{-1} under the conditions of Figure 4) is too slow to fit the rapid loss of phosphoenzyme observed, so that the rate of this step must also be increased.

This combination of effects, a decrease in the effective rate of the E2–E1 transition with a corresponding increase in the effective equilibrium constant E2/E1 in favor of E2, an increase in the effective rate of dephosphorylation with a corresponding decrease in the effective equilibrium constant for phosphorylation from P_i, and an increase in the effective rate of the Ca_2E1P–E2P transition, allows us to fit all our data on the effects of nonylphenol. Multiple effects are to be expected since if nonylphenol changes the equilibrium constant for any one step, then the equilibrium constant for at least one other step must also be changed, since the product of the equilibrium constants for all the steps around the reaction cycle must remain constant (corresponding to the simple hydrolysis of ATP to ADP and P_i).

In the simulations to be described, the parameters are as given previously (Gould et al., 1986; Stefanova et al., 1987) with the exceptions described above; full details will be pub-

lished elsewhere (Michelangeli, East, and Lee, unpublished results). For these simulations we have assumed the slow step in the Ca_2E1P–E2P sequence to be the Ca_2E1P–Ca_2E2P step, but equally good fits to the data can be obtained by assuming the slow step to be Ca_2E2P–E2P. As reported previously (Gould et al., 1986), ratios of ATPase activities measured at high and low concentrations of MgATP differ between preparations, which we have attributed to different levels of stimulation of the rate of the Ca_2E1P–E2P transition by bound MgATP (Gould et al., 1986). Table III lists the parameters that need to be changed to simulate the effects seen with nonylphenol. The major effect is on the effective rate of the E2–E1 transition and on the effective rate of the corresponding transition for the MgATP-bound forms, E2MgATP–E1MgATP.

The effect of nonylphenol on ATPase activity (Figure 3) can be fitted by assuming that the effective rates of the E2–E1 transitions for the MgATP-free and MgATP-bound forms decrease to 0.07 and 5.66, respectively, with a binding constant of 0.5 mM for MgATP to E2, with 10- and 7-fold increases in the effective rates of the Ca_2E1P–Ca_2E2P transition and dephosphorylation, respectively (Table III). The experimental data on the rate of phosphorylation of SR by 5 μM MgATP in the absence of nonylphenol are well fitted by the parameters given in Table III (Figure 4). The effect of 100 μM nonylphenol on SR at a protein concentration of 0.1 mg/mL can be simulated by using the values for the rates of the E2–E1 transition used above but with 20- and 15-fold increases in the effective rates of the Ca_2E1P–E2P transition and dephosphorylation, respectively (Figure 4). An increase in the effective rate of dephosphorylation caused by nonylphenol would suggest a decrease in the effective equilibrium constant for phosphorylation by P_i. Such a decrease was observed experimentally, the effect of 12 μM nonylphenol at a protein concentration of 0.3 mg/mL being consistent with a 7.7-fold decrease in the effective equilibrium constant for phosphorylation (Figure 5).

It has been suggested that the E2–E1 step can be studied by observation of the fluorescein fluorescence of the ATPase labeled with FITC (Pick, 1982; Froud et al., 1986b). Addition of Ca^{2+} results in a small decrease in fluorescence intensity attributed to the E2–E1 transition, the magnitude of the change giving the proportion of the ATPase in the E2 state (Froud et al., 1986b). The rate of change is too fast to follow accurately in manual mixing experiments (Figure 7). The magnitude of the response to Ca^{2+} increases on addition of nonylphenol, the effect being particularly marked at pH 7 (Figure 7). The changes in the response to Ca^{2+} in the presence of nonylphenol relative to those in its absence can be simulated by using the equations in Gould et al. (1986) and are consistent with a 7-fold increase in the effective E2/E1 equilibrium constant on addition of nonylphenol. The rate of the E2–E1 transition is pH dependent and can be calculated as in Gould et al. (1986) and Stefanova et al. (1987). Figure 7 shows that the rate of the response to Ca^{2+} becomes slower on addition of nonylphenol, particularly at pH 6. By use of the constants given in Gould et al. (1986), the effective E2–E1 rate of 0.07 at pH 7.2 used to fit the ATPase activity data (Figure 3) corresponds to rates of 0.05 and 0.01 at pH 7 and pH 6, respectively, and, as shown in Figure 7, these rates give a good fit to the experimentally determined rates of the Ca^{2+} responses at these pH values.

An increase in the effective E2/E1 equilibrium constant would be expected to decrease the apparent affinity of the ATPase for Ca^{2+}, since only the E1 form has high affinity for Ca^{2+}. Binding of Ca^{2+} to the ATPase can be studied by observation of the tryptophan fluorescence of the ATPase, since addition of Ca^{2+} to the ATPase results in an increase in tryptophan fluorescence intensity, with the E2, E1, and CaE1 forms of the ATPase having relatively low fluorescence intensities and the CaE1′ and Ca_2E1' forms having higher fluorescence intensities (Fernandez-Belda et al., 1984). A model describing Ca^{2+} binding to the ATPase has been presented in Gould et al. (1986). The Ca^{2+}-dependent effects reported by Pitithory and Jencks (1988) can be fitted with effective equilibrium constants of 1.9×10^5, 0.15, and 6.78×10^6 for the E1 + $Ca^{2+} \rightleftharpoons$ CaE1, CaE1 $\rightleftharpoons$ CaE1′, and CaE1′ + $Ca^{2+} \rightleftharpoons$ Ca_2E1 steps, respectively, at pH 7 (data not shown). When our pCa values are corrected by 0.5 to account for the different Ca^{2+}-EGTA binding constant used by Petithory and Jencks (1988), the tryptophan response to Ca^{2+} can be fitted well by using the above binding constants, assuming that the fluorescence of the high-fluorescence forms is 6% greater than that of the low-fluorescence forms (Figure 8). In the presence of nonylphenol the affinity of the ATPase for Ca^{2+} is reduced, and the experimental data are fitted well by a 7-fold increase in the effective E2/E1 equilibrium constant (Figure 8), together with an increase in the magnitude of the fluorescence response to Ca^{2+} to 10%. As shown in Figure 2, these same binding parameters fit the Ca^{2+} dependence of ATPase activity (with the rate parameters given in Table III, except that for this lower activity preparation of ATPase the stimulation of the rate of the Ca_2E1P–E2P step by MgATP is only 5-fold). In agreement with the experimental data, the calculated dependence of ATPase activity on the concentration of Ca^{2+} is only slightly dependent on the value of the E2/E1 ratio, because strong binding of MgATP to E1 strongly favors E1MgATP over E2.

Increases in the effective rates of the Ca_2E1P–E2P step and of dephosphorylation, together with a large decrease in the effective rate of the E2–E1 step, would result in a large buildup of the E2 form of the ATPase at steady state in the presence of nonylphenol, which should be detected by changes in tryptophan fluorescence intensity. The fluorescence response of the ATPase to addition of Ca^{2+} and MgATP is usually complex, because of the formation of many intermediates at steady state, each with potentially different fluorescence intensities (Champeil et al., 1986). Nevertheless, the largest change in tryptophan fluorescence intensity seems to correspond to that between the low-fluorescent form E2 and the high-fluorescent form Ca_2E1, as described above. Addition of Ca^{2+} to the ATPase in the absence of nonylphenol results in a 6% increase in fluorescence intensity, and subsequent addition of MgATP results in a small and transitory decrease in fluorescence intensity (Figure 9). Simulations show that under these conditions at steady state the ATPase is predominantly present in the Ca_2E1P, E2P, and Ca_2E1 forms, with little E2 present. On addition of nonylphenol, the fluorescence response to Ca^{2+} becomes larger and slower and the response to MgATP also increases in magnitude to become almost equal in size to that on addition of Ca^{2+}; the response also becomes much longer lasting (Figure 9). Simulations show a very large increase in E2 at steady state under these conditions, and the experimental data can be simulated well with the rate constants given in Table III by assuming that the decrease in fluorescence is directly proportional to the fraction of the ATPase in the E2 form and using the fluorescence response to Ca^{2+} at each particular concentration of nonylphenol to calibrate the magnitude of the fluorescence change due to the formation of E2.

A buildup of ATPase in the E2 form at steady state should also be detectable by a large increase in the amount of Ca^{2+} released by the ATPase on addition of MgATP (Table II). The level of Ca^{2+} bound to the ATPase adsorbed onto a filter was ca. 10 nmol/mg of protein which, for binding of 2 mol of Ca^{2+}/mol of ATPase, would correspond to 60% active ATPase, in agreement with the maximal level of phosphorylation ($[EP]_{max}/[E]_{total}$) of 0.6 for this preparation of ATPase. On addition of MgATP, the level of bound Ca^{2+} was observed to decrease, the amount of Ca^{2+} released being greater in the presence of nonylphenol than in its absence, at both pH 6 and 7 (Table II). Addition of nonylphenol also resulted in a decrease in the measured level of Ca^{2+} binding to the ATPase in the absence of MgATP, which might reflect some denaturation of the ATPase in the presence of nonylphenol and absence of MgATP when absorbed to the filters. Simulations with the parameters given in Table III give levels of bound Ca^{2+} in good agreement with the experimental data (Table II).

Effects of BHT on the ATPase are less marked than those of nonylphenol. As shown in Figure 5, BHT has no effect on phosphorylation, suggesting that it does not affect the equilibrium constant or the rate constant for dephosphorylation. The effect of BHT on ATPase activity can, in fact, be simulated by assuming no effect on either dephosphorylation or the Ca_2E1P–$E2P$ step, but with a reduction in the effective rates of the E2–E1 step for the MgATP-free and MgATP-bound forms to 0.4 and 33.0, respectively, at pH 7.2 (Figure 3). The corresponding rates for the E2–E1 step at pH 7 and 6 are 0.28 and 0.07, respectively, and, together with an increase in the effective equilibrium constant E2/E1 by a factor of 7 as observed for nonylphenol, these give reasonable simulations of the observed change in fluorescein fluorescence of FITC-labeled SR on addition of Ca^{2+} (Figure 7).

As with a variety of other hydrophobic molecules (Lee, 1987), the effects of phenols reported above depend on the phospholipid present in the system. For the ATPase reconstituted with DOPC, effects on ATPase activity are comparable to those with the native ATPase (Figure 10). For the ATPase reconstituted with DMPC, however, addition of low concentrations of the phenols results in a very large increase in activity, to above that seen with DOPC. At higher concentrations, inhibition occurs for the ATPase reconstituted with both DOPC and DMPC (Figure 10). Table IV shows that these effects do not follow from binding at the lipid–protein interface on the ATPase, since addition of the phenols to the ATPase reconstituted with the quenching lipid BrPC results in no increase in tryptophan fluorescence intensity. A variety of other molecules that increase the activity of the ATPase reconstituted with DMPC have also been shown not to bind to the ATPase at the lipid–protein interface (annular sites), and it has been proposed that such molecules bind to other sites on the ATPase (nonannular sites), either at protein–protein interfaces between dimers or higher aggregates of the ATPase or within the ATPase molecule (Lee, 1987). Finally, we can conclude that the effects of nonylphenol do not follow from effects on viscosity, since nonylphenol modifies equilibrium constants for a number of steps in the reaction sequence (Lee et al., 1989). The suggested increase in the E2/E1 ratio and decrease in the rate of the E2–E1 transition suggests that nonylphenol may interact preferentially with the E2 form of the ATPase, stabilizing that form. Stabilization of E2 could also explain the decrease in the equilibrium constant for phosphorylation of the ATPase by P_i.

ACKNOWLEDGMENTS

We thank K. Waterloh for preliminary experiments.

Registry No. ATPase, 9000-83-3; BHT, 128-37-0; nonylphenol, 25154-52-3.

REFERENCES

Almeida, L. M., Vaz, W. L. C., Stumpel, J., & Madeira, V. M. C. (1986) *Biochemistry 25*, 4832–4839.

Bishop, J. E., & Al-Shawi, M. K. (1988) *J. Biol. Chem. 263*, 1886–1892.

Cha, S. (1968) *J. Biol. Chem. 243*, 820–825.

Champeil, P., & Guillain, F. (1986) *Biochemistry 25*, 7623–7633.

Champeil, P., Le Maire, M., Moller, J. V., Riollet, S., Guillain, F., & Green, N. M. (1986) *FEBS Lett. 206*, 93–98.

Chance, E. M., Curtis, A. R., Jones, I. P., & Kirby, C. R. (1977) FACSIMILE: A Computer Program for Flow and Chemistry Simulation, HMSO, London.

Chong, P. L. G., Fortes, P. A. G., & Jameson, D. M. (1985) *J. Biol. Chem. 260*, 14484–14490.

Coll, R. J., & Murphy, A. J. (1984) *J. Biol. Chem. 259*, 14249–14254.

de Foresta, B., le Maire, M., Orlowski, S., Champeil, P., Lund, S., Moller, J. V., Michelangeli, F., & Lee, A. G. (1989) *Biochemistry 28*, 2558–2567.

de Meis, L., & Vianna, A. (1979) *Annu. Rev. Biochem. 48*, 275–292.

Dupont, Y. (1978) *Biochem. Biophys. Res. Commun. 71*, 893–900.

East, J. M., & Lee, A. G. (1982) *Biochemistry 21*, 4144–4151.

East, J. M., Jones, O. T., Simmonds, A. C., & Lee, A. G. (1984) *J. Biol. Chem. 259*, 8070–8071.

Fernandez-Belda, F., Kurzmack, M., & Inesi, G. (1984) *J. Biol. Chem. 259*, 9687–9698.

Froud, R. J., & Lee, A. G. (1986) *Biochem. J. 237*, 207–215.

Froud, R. J., East, J. M., Rooney, E. K., & Lee, A. G. (1986a) *Biochemistry 25*, 7535–7544.

Froud, R. J., East, J. M., Jones, O. T., & Lee, A. G. (1986b) *Biochemistry 25*, 7544–7552.

Gould, G. W., East, J. M., Froud, R. J., McWhirter, J. M., Stefanova, H. I., & Lee, A. G. (1986) *Biochem. J. 237*, 217–227.

Guillain, F., Champeil, P., & Boyer, P. D. (1984) *Biochemistry 23*, 4754–4761.

Hardwicke, P. M. D., & Green, N. M. (1974) *Eur. J. Biochem. 42*, 183–193.

Jones, O. T., & Lee, A. G. (1986) *Pestic. Biochem. Physiol. 25*, 420–430.

Lee, A. G. (1987) *J. Bioenerg. Biomembr. 19*, 581–603.

Lee, A. G., East, J. M., Jones, O. T., McWhirter, J., Rooney, E. K., & Simmonds, A. C. (1982) *Biochemistry 21*, 6441–6446.

Lee, A. G., Michelangeli, F., & East, J. M. (1989) *Biochem. Soc. Trans. 17*, 962–964.

Leo, A., Hansch, C., & Elkins, D. (1971) *Chem. Rev. 71*, 525–573.

Meissner, G., Conner, G. E., & Fleischer, S. (1973) *Biochim. Biophys. Acta 298*, 246–269.

Petithory, J. R., & Jencks, W. P. (1988) *Biochemistry 27*, 5553–5564.

Pick, U. (1982) *J. Biol. Chem. 257*, 6111–6119.

Rooney, E. K., Gore, M. G., & Lee, A. G. (1987) *Biochemistry 26*, 3688–3697.

Segal, I. H. (1975) *Enzyme Kinetics*, Wiley, New York.

Shigekawa, M., & Dougherty, J. P. (1978) *J. Biol. Chem. 253*, 1458–1464.

Simmonds, A. C., East, J. M., Jones, O. T., Rooney, E. K., McWhirter, J., & Lee, A. G. (1982) *Biochim. Biophys. Acta 693*, 398-406.
Sinensky, M. (1974) *Proc. Natl. Acad. Sci. U.S.A. 71*, 522-525.
Sokolove, P. M., Albuquerque, E. X., Kauffman, F. C., Spande, T. F., & Daly, J. W. (1986) *FEBS Lett. 203*, 121-126.
Stahl, N., & Jencks, W. P. (1987) *Biochemistry 26*, 7654-7667.
Stefanova, H. I., Napier, R. M., East, J. M., & Lee, A. G. (1987) *Biochem. J. 245*, 723-730.
Wakabayashi, S., Ogurusu, T., & Shigekawa, M. (1986) *J. Biol. Chem. 261*, 9762-9769.

Analysis of the Active Site of the Flavoprotein *p*-Hydroxybenzoate Hydroxylase and Some Ideas with Respect to Its Reaction Mechanism†

Herman A. Schreuder,* Wim G. J. Hol, and Jan Drenth
Laboratory of Chemical Physics, Nijenborgh 16, 9747AG Groningen, The Netherlands
Received January 17, 1989; Revised Manuscript Received November 16, 1989

ABSTRACT: The flavoprotein *p*-hydroxybenzoate hydroxylase has been studied extensively by biochemical techniques by others and in our laboratory by X-ray crystallography. As a result of the latter investigations, well-refined crystal structures are known of the enzyme complexed (i) with its substrate *p*-hydroxybenzoate and (ii) with its reaction product 3,4-dihydroxybenzoate and (iii) the enzyme with reduced FAD. Knowledge of these structures and the availability of the three-dimensional structure of a model compound for the reactive flavin 4a-hydroperoxide intermediate has allowed a detailed analysis of the reaction with oxygen. In the model of this reaction intermediate, fitted to the active site of *p*-hydroxybenzoate hydroxylase, all possible positions of the distal oxygen were surveyed by rotating this oxygen about the single bond between the C4a and the proximal oxygen. It was found that the distal oxygen is free to sweep an arc of about 180° in the active site. The flavin 4a-peroxide anion, which is formed after reaction of molecular oxygen with reduced FAD, might accept a proton from an active-site water molecule or from the hydroxyl group of the substrate. The position of the oxygen to be transferred with respect to the substrate appears to be almost ideal for nucleophilic attack of the substrate onto this oxygen. The oxygen is situated above the 3-position of the substrate where the substitution takes place, at an angle of about 60° with the aromatic plane, allowing strong interactions with the π electrons of the substrate. Polarization of the peroxide oxygen–oxygen bond by the enzyme may enhance the reactivity of flavin 4a-peroxide.

Flavoprotein monooxygenases have been the subject of intensive studies. Members of this class of enzymes are *p*-hydroxybenzoate hydroxylase and other phenolic hydroxylases, bacterial luciferase, and microsomal flavin-dependent monooxygenase. These enzymes share the unique property that they are able to break the double bond of molecular oxygen and incorporate one oxygen in a substrate without the help of a metal ion as a catalyst (Bruice, 1984b). The other oxygen of the dioxygen molecule is converted into water. The way in which the flavin prosthetic group is able to activate molecular oxygen has received much attention [see, for instance, Wessiak et al. (1984b) and Bruice (1984a)].

p-Hydroxybenzoate hydroxylase is a well-studied example of a flavin-containing monooxygenase. It converts *p*-hydroxybenzoate into 3,4-dihydroxybenzoate with the help of molecular oxygen and NADPH. From biochemical studies (Entsch et al., 1976a; Husain & Massey 1979; Shoun et al., 1979b), the reaction scheme shown in Figure 1 has emerged.

The amino acid sequence of the enzyme from *Pseudomonas fluorescens*, which contains 394 residues, is known (Hofsteenge et al., 1983; Weijer et al., 1982; Wijnands et al., 1986). Chemical modification studies (Van Berkel et al., 1984; Wijnands et al., 1986), nuclear magnetic resonance studies (Vervoort, 1986), and studies of model reactions (Anderson et al., 1987; Bruice, 1984b; Wessiak et al., 1984a) have given further insights in the catalytic pathway. In our laboratory, the structure of the *Pseudomonas fluorescens* *p*-hydroxybenzoate hydroxylase enzyme–substrate (ES)[1] complex in the oxidized state was elucidated by Wierenga et al. (1979) and has recently been refined at 1.9-Å resolution (Schreuder et al., 1989). Lower resolution structures of the substrate-free complex, the reduced enzyme–substrate (ES_{red}) complex, and the enzyme–product (EP) complex have been obtained (Van der Laan, 1986; Schreuder et al., 1987, 1988a). Some of these crystal structures will now be analyzed to find out which factors might contribute to the catalysis of the hydroxylation step.

We will particularly focus our attention on the flavin 4a-peroxide intermediate (Figure 1, intermediate 5; Figure 2a) and the flavin 4a-hydroxide. The first intermediate has been shown to occur a few milliseconds before the actual hydroxylation step, the second intermediate a few milliseconds after the hydroxylation reaction (Entsch et al., 1976a). The

†This research has been carried out under the auspices of The Netherlands Foundation for Chemical Research (SON) with financial aid from The Netherlands Organization for Scientific Research (NWO).

[1] Abbreviations: enzyme, *p*-hydroxybenzoate hydroxylase; substrate, *p*-hydroxybenzoate; product, 3,4-dihydroxybenzoate; ES, enzyme–substrate; ES_{ox}, oxidized ES; ES_{red}, reduced ES; EP, enzyme–product; Sol, solvent molecule.

0006-2960/90/0429-3101$02.50/0